

## Investigation of Protective Effect of Polymeric Film Coatings on Carbon Steel in Aggressive Solutions

Florina Branzoi<sup>1,\*</sup> and Viorel Branzoi<sup>2</sup>

<sup>1</sup> Institute of Physical Chemistry “Ilie Murgulescu” 202 Splaiul Independenței, 060021 Bucharest, Romania

<sup>2</sup> Department of Applied Physical Chemistry and Electrochemistry, University Politehnica of Bucharest, 132 Calea Grivitei, 010737 Bucharest, Romania

\*E-mail: [fbranzoi@chimfiz.icf.ro](mailto:fbranzoi@chimfiz.icf.ro)

Received: 8 April 2016 / Accepted: 26 May 2016 / Published: 7 July 2016

---

In this paper, galvanostatic electropolymerization technique has been used for to obtain of new composite (PPY-SDS/PNNDMA and PNNDMA/ PPY-SDS) coatings onto carbon steel of type OL 37 for corrosion protection. Monolayer poly (N, N' dimethylaniline) (PNNDMA), polypyrrole (PPY), and bilayer PNNDMA/PPY-SDS and PPY-SDS/PNNDMA coatings were electrodeposition on carbon steel by galvanostatic methods from synthesis solutions 0.1 M N,N' dimethylaniline, 0.1M pyrrole, 0.01 M sodium dodecyl sulfate (SDS) with 0.3M H<sub>2</sub>C<sub>2</sub>O<sub>4</sub>. It was used dodecylsulfate ions as dopant to polypyrrole, SDS has been likewise introduced into the synthesis solution of polypyrrole. The properties of monolayer and bilayer composite polymer have been realized out by electrochemical voltammetry, FT-IR analysis and SEM measurements. The anticorrosive properties of the OL37 coated has been studied by electrochemical polarization and EIS measurements in 0.5M H<sub>2</sub>SO<sub>4</sub> medium. The analysis of the corrosion protection samples demonstrated that PNNDMA/PPY-SDS coatings assure a great anticorrosive performance of carbon steel in corrosive environments. Bilayer composite polymer showed greater corrosion protection effectiveness compared to monolayer composite polymer.

---

**Keywords:** nanocomposite films, galvanostatic electrodeposition, corrosion protection, SEM, EIS, FT-IR

### 1. INTRODUCTION

Carbon steel, the most widely used engineering material, is about 85% of the annual production of steel world at range [1]. Carbon steel is used in great tonnes in chemical processing, construction and metal –processing equipment, in marine applications and petroleum production and refining [1]. Carbon steel is utilized in numerous practices; this intensified the study in corrosion strength in different corrosive media [1]. Numerous methods there are to improve the corrosion resistance of the

carbon steel utilized as mechanical components in industry [2-8]. The use of galvanostatic polymerization technique, nanostructured coatings, applying organic, metallic or inorganic coatings, cathodic and anodic protection are methods for metals and alloys corrosion protection. The corrosion protection of coatings based on electrodeposited polymers was studied in the recent years and their application for protection of many metals and alloys: carbon steel, zinc, copper, brass and other metals was reported. [2-9]. Organic coatings have long been used to protect metals and alloys against corrosion. The primary effect of an organic coating is to act as a barrier against an aggressive species [7-8, 9-12]. Moreover, for all organic coatings pathways will be created for the corrosive species to reach substrate and localized corrosion will occur. Few researches regarding to the use of conducting polymer coatings onto metal for corrosion protection were presented in the last years [9-13]. The composite based conducting polymer like polyaniline and polypyrrole on carbon steel electrode were achieved by electrochemical polymerization and these composite films ensure significant protecting properties at corrosion [7-8-12-16]. Now, the polymers have assumed an importance as anticorrosion layers for many metallic materials [8 -18]. The electropolymerization is easy enough inexpensive and most suitable way for synthesis of novel composite films over metallic materials. Few researches were achieved and related on the protective behavior of conducting and insulating forms of polymers on various materials [8, 10-14 and 17-30].

In this paper, it were investigated two conducting polymers, in the main as polymeric coatings on OL 37 surface with monolayers of Poly N, N' dimethylaniline (NNDMA) and polypyrrole (PPY) and then bilayer polymeric coatings like PPY-SDS/NNDMA and NNDMA/PPY-SDS what have been electrodeposited over carbon steel surface by galvanostatic methods from aqueous solutions of 0.1 M N, N' dimethylaniline, 0.1M pyrrole, 0.01 M sodium dodecyl sulfate (SDS) and 0.3 M H<sub>2</sub>C<sub>2</sub>O<sub>4</sub>. The properties of monolayer and bilayer composite polymer have been achieved with electrochemical voltammetry, Fourier transform infrared (FT-IR) analysis and scanning electron microscopy (SEM) methods. Anticorrosion protection of PPY-SDS/PNNDMA and PNNDMA/ PPY-SDS coated has been studied by electrochemical polarization and electrochemical impedance spectroscopy (EIS) methods in 0.5 M H<sub>2</sub>SO<sub>4</sub> solutions.

## 2. EXPERIMENTAL

All chemicals have been reagent grade, N, N' dimethylaniline (NNDMA), pyrrole (PPY), have been provide from Fluka, acid oxalic dehydrate (H<sub>2</sub>C<sub>2</sub>O<sub>4</sub>) was received from Merck. In all measurements, the synthetic solutions have been realized with bidistilled water: NNDMA 0.1M, SDS 0.01M, PPY 0.1M and 0.3M H<sub>2</sub>C<sub>2</sub>O<sub>4</sub>. The composition of the working electrode type OL 37 is: C% 0.15, Si 0.09%, Mn 0.4 %, Fe% 99.293, P% 0.023, S% 0.02, Al% 0.022, Ni % 0.001 and Cr% 0.001. All electrochemical measurements and electrochemical impedance spectroscopy techniques have been performed by using a single –compartment cell with the standard three electrodes set up at temperature 25<sup>0</sup>C. The cell was connected to a VoltaLab potentiostat coupled to a PC with VoltaMaster software. As working electrode it was used a carbon steel of type OL 37 with the cylindrical shape and with area of 0.5 cm<sup>2</sup>, Pt sheet as auxiliary electrode and saturated calomel electrode (SCE) as reference

electrode. Previously every measurement, the samples was polished with a series of sandpapers of varied granulation sizes (250 to 4500 grids) up to mirror-luster. After polishing, the OL 37 electrode has been cleaning with acetone and doubly distilled water, dried at room temperature and introduced in the electrochemical cell, which has been the conventional three-electrode cell [8-11, 20]. Experimental techniques were described in previous papers [8-11]. Before electrodeposition of polymer coatings, the OL 37 working electrode has been passivated in 0.3M  $\text{H}_2\text{C}_2\text{O}_4$  medium by electrochemical voltammetry at the interval potential of -500mV up to 1600 mV versus SCE at a sweep rate 20mV/s. The coatings at the conducting polymers from the synthesis solution of monomer 0.1M NNDMA, 0.1M-PPY and 0.01M SDS in 0.3 M  $\text{H}_2\text{C}_2\text{O}_4$  were deposited onto OL 37 surface of the passivated carbon steel electrode, from 0.3M  $\text{H}_2\text{C}_2\text{O}_4$  [8-14, 20-24]. The electrosynthesis has been performed by galvanostatic methods: the monolayer at current densities  $0.5\text{mA}/\text{cm}^2$  for NNDMA,  $10\text{mA}/\text{cm}^2$  for PPY-SDS and bilayer at  $1\text{mA}/\text{cm}^2$  for PPY-SDS/NNDMA (NNDMA over PPY-SDS) and at  $10\text{mA}/\text{cm}^2$  for NNDMA/PPY-SDS (PPY-SDS over NNDMA), the electrodeposition of every film has been permitted for 900 seconds. Afterwards which electrodeposition, the OL 37 electrode has been taken out from the synthesis solution and washed with bidistilled water and dried in atmosphere. The electrochemical behavior (electroactivity) of composite polymer has been analyzed in a medium of 0.3 M  $\text{H}_2\text{C}_2\text{O}_4$ . The composite structure has been established utilizing Bruker FT-IR spectrometer with ATR in the spectral interval  $4000\text{-}650\text{cm}^{-1}$ . SEM has been used to analyze the morphological structure with JEOL JSM-5500LV microscope. The anticorrosive properties of the OL 37 coated has been studied by electrochemical polarization and electrochemical impedance spectroscopy (EIS) measurements in 0.5M  $\text{H}_2\text{SO}_4$  solutions. Analysis of Tafel polarization curves has been realized by scanning the potential from cathodic to anodic potentials in regarding to OCP-open circuit potential at a scan rate of 2mV/s. Electrochemical impedance spectroscopy methods have been achieved in the frequency interval of 100 kHz to 40 mHz with amplitude 10mV at the OCP of PPY-SDS, PNNDMA, PNNDMA/PPY-SDS and PPY-SDS/ PNNDMA uncoated and coated electrodes [7, 8-12].

### 3. RESULTS AND DISUSSION

The cyclic voltammograms registered at the passivation of carbon steel electrode in 0.3M  $\text{H}_2\text{C}_2\text{O}_4$  solution is presented in figure 1. This method of OL 37 electrode passivated prior electrodeposition method it has been related as well, in specialty literature. [8, 9-12-22].

The passivation process is realized on the obtaining of the insoluble compounds over the electrode surface. These insoluble compounds formed of iron oxides, insoluble iron oxalates such as  $\text{Fe}(\text{Ox})$  and  $\text{FeC}_2\text{O}_4^-$ . These conditions determine the passivation of the OL 37 electrode by obtain of a thin insoluble iron oxalate layer which prevents metal dissolution without impeding the electrodeposition process [7-8, 9-14, 26-39]. The improving of the electrodeposition conditions establish at electrodeposition of NNDMA or PPY layers which have the excellent anticorrosive properties. From examination of the figure 1, it can be noted that, at the first cycle on the anodic bough is observed a greater and high oxidation peak at the potential -304 mV and at the current density of  $20.6\text{mA}/\text{cm}^2$  which indicates out that dissolution of Fe started and because the dissolution mechanism

it is very high now and as well, which in this reaction results  $Fe^{2+}$  ions in its immediate and second anodic peak is at potential 145 mV and at current density of  $130\text{mA}/\text{cm}^2$  [8-28-31]. These ions interact with the oxalate electrolyte to form insoluble  $FeC_2O_4$ . These ions react with the oxalate electrolyte to obtain insoluble  $FeC_2O_4$  [8-12-16, 24-30]

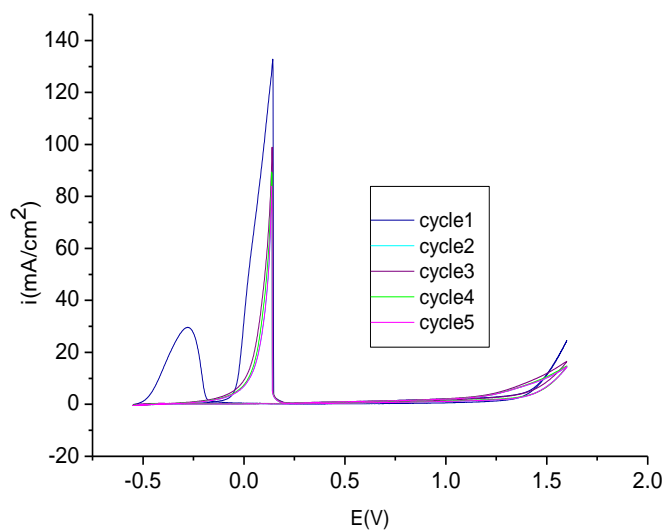


**Figure 1.** The voltammograms registered at the polarization of OL 37 electrode in 0.3M  $H_2C_2O_4$  solution at the potential interval of -500 to 1600mV at scan rate 20mV/s

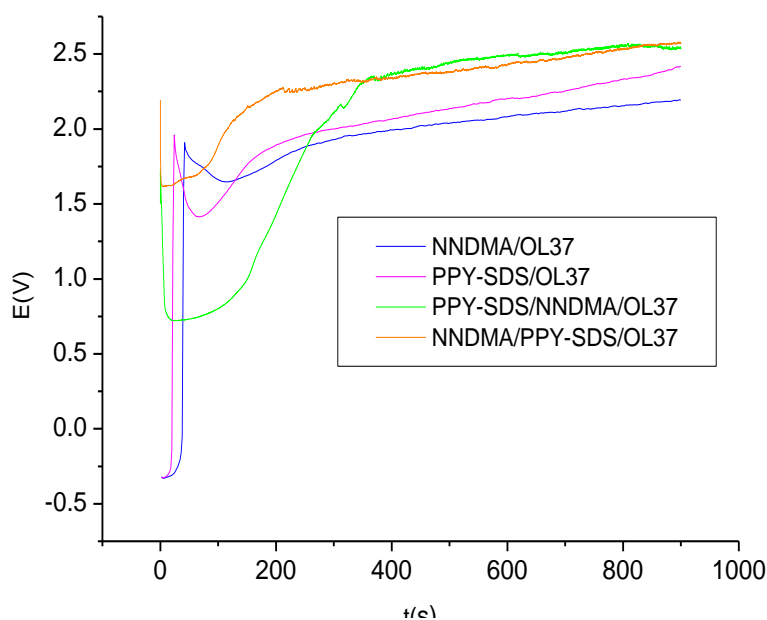


**Figure 2.** Galvanostatic deposition of PPY-SDS/OL37, NNDMA/OL37, PPY-SDS on the NNDMA/OL37 (monolayer) and NNDMA over the PPY-SDS/OL37 with obtaining of a bilayer

The polymer coatings have been performed at galvanostatic conditions as well were presented above. Figure 2 represent the potential-times curves realized during the deposition of the polymeric film as: polypyrrole –sodium dodecylsulfate on carbon steel OL37 (PPy-SDS/OL37), N, N' dimethylaniline on carbon steel OL37(NNDMA/OL37), N N' dimethylaniline over polypyrrole–sodium dodecylsulfate (PPY-SDS/NNDMA/OL37) and polypyrrole–sodium dodecylsulfate over N N' dimethylaniline (NNDMA/PPY-SDS/OL37) with formation of a bilayer and coating at 1mA and 10mA/cm<sup>2</sup> over the OL 37 area where prior has been electrodeposited monolayer N, N' dimethylaniline at 0.5mA/cm<sup>2</sup> and polypyrrole–sodium dodecylsulfate at 10mA/cm<sup>2</sup>.

The electrodeposition process can be interpreted by a nucleation phenomenon which establish to polymer grains on OL 37 surface [8, 10]. It can be seen from figure 2, deposition of NNDMA, PPy-SDS coatings on OL 37 the time nucleation increases with increasing the potential. Anyway, the potential remains constant at values corresponding to the monomer oxidation and the electropolymerization process starts [5-12]. Induction period as smaller than 100s has been noticed for the electropolymerization of PPy and NNDMA films and its value decreased with increasing the current density and the increase of the nucleation potential. The coating PNNDMA over the PPy-SDS (monolayer) is described by a sharp increase through a most positive amount, then the potential stabilizes to a steady value. About the galvanostatic electrodeposition of PNNDMA film at 1mA/cm<sup>2</sup> on the PPy-SDS/OL37 coated OL 37, potential instantly end up at the value corresponding to the electropolymerization method. The observed of OL 37 electrode after galvanostatic deposition of PPy-SDS/NNDMA/OL 37, and NNDMA/PPY-SDS/ OL 37 coated indicates the obtaining of a black coloured coating and this coating is uniform, smooth and adherent at the electrode surface type OL 37 [7, 10, 12, 24, 38].

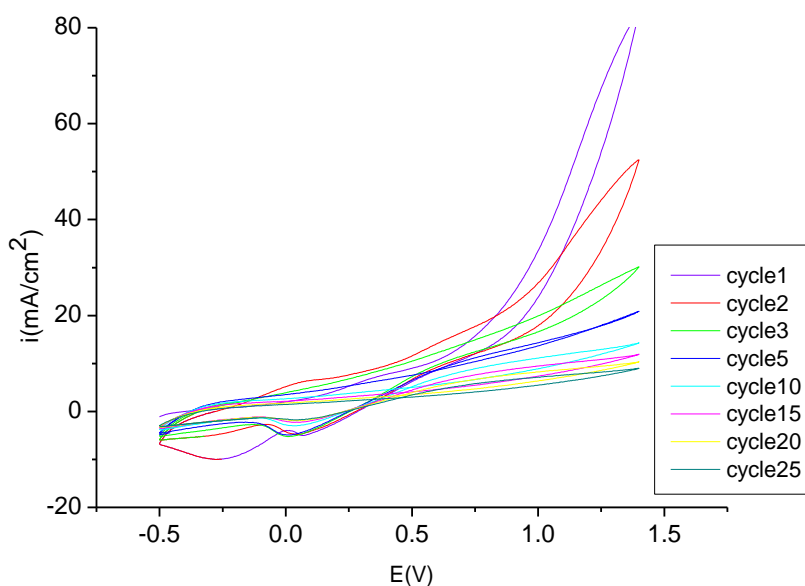


**Figure 3.** Cyclic voltammograms of OL 37 electrodes coated with PPY-SDS/NNDMA/OL 37 bilayer in 0.3M H<sub>2</sub>C<sub>2</sub>O<sub>4</sub> solution monomer-free at potential interval -0.5 and 1.5V vs. SCE and sweep rate of 20mV/s

The current –potential behaviour of PPY-SDS/NNDMA/OL 37 coated on carbon steel electrode in 0.3M  $\text{H}_2\text{C}_2\text{O}_4$  solution monomer free is shown in figure 3 and NNDMA/PPY-SDS/ OL 37 coated is presented in figure 4 at potential interval of -0.5 and +1.5V vs. SCE at sweep rate of 20mV/s. Analyzing these figures (3-4), it can be seen that the electrochemical behavior of coating polymeric film changes with the number of cycles and with electropolymerization conditions.

The stability of any conducting polymer in reduced and oxidized states is a significant characteristic for many practices [7-14]. The principal cause that establishes the lifecycle of a conducting polymer is a chemical permanency of the matrix itself. The steadiness of PPY-SDS/NNDMA/OL 37 and NNDMA/PPY-SDS/ OL 37 bilayer coating has been determined by electrochemical voltammetry (up 20 cycles) in oxalic acid medium (monomers- free, in figure 3 and figure 4). The presence of oxidation and reduction wave after several cycles (up 10) exhibit the steadiness of this electroactive polymeric layer [7-12, 32-36, 38-43]. When cycling take place the current density decreases with each cycle and at last achieve at a constant value.

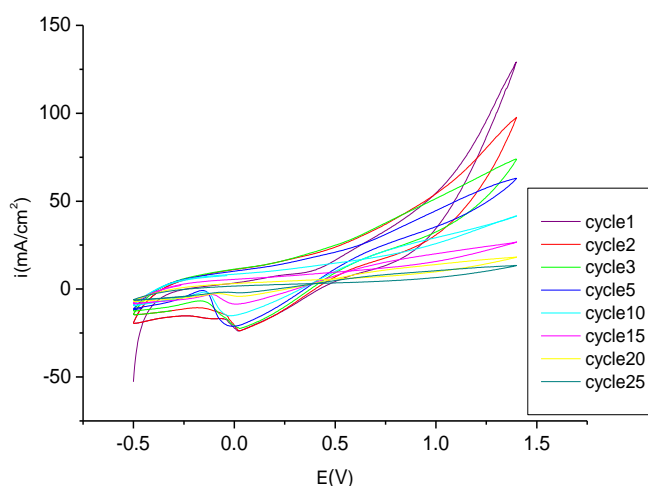
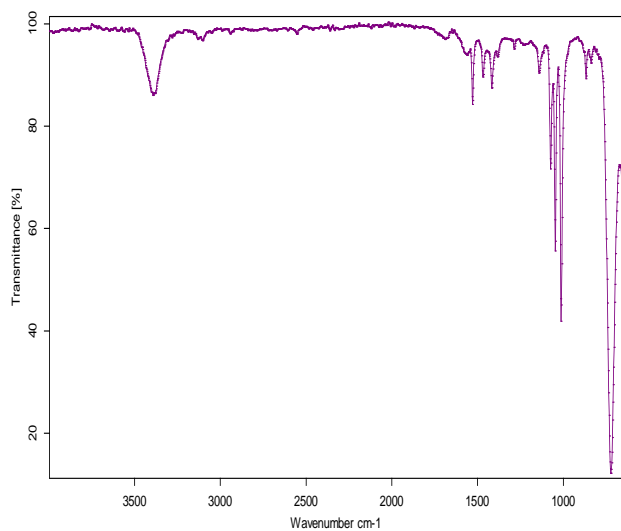
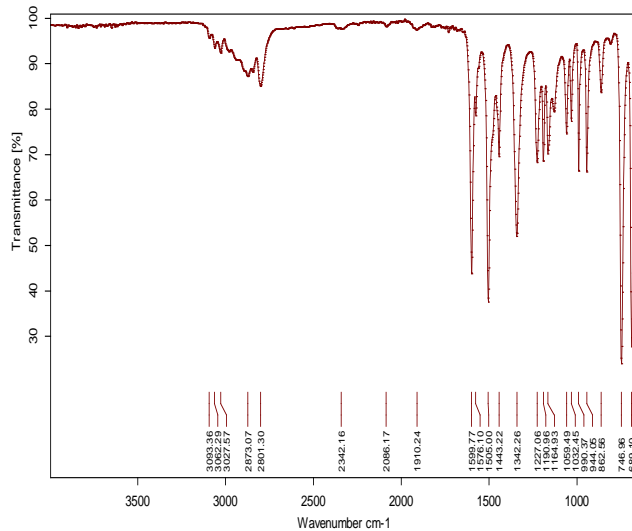


**Figure 4.** Voltammograms of OL 37 coated with NNDMA/PPY-SDS/ OL 37 bilayer in 0.3M  $\text{H}_2\text{C}_2\text{O}_4$  solution monomer free at potential interval -0.5 and 1.5V vs. SCE and sweep rate of 20mV/s

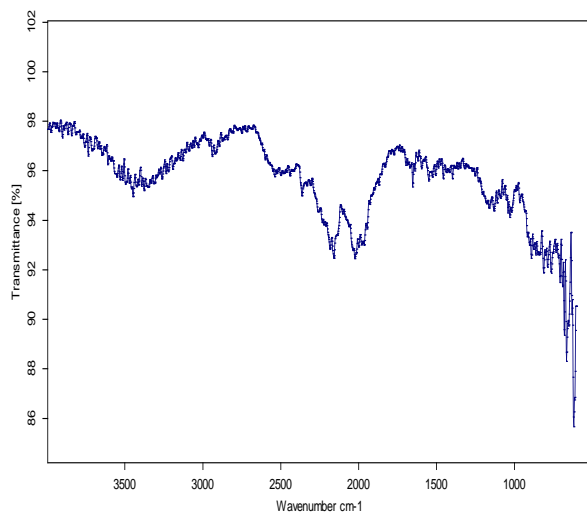
Fourier transform infrared (FT-IR see figure 5) spectra have been performed with a Bruker optics spectrometer at room temperature. All spectra in this study have been realized at a resolution  $4\text{cm}^{-1}$  in the region  $4000\text{-}650\text{cm}^{-1}$  FT-IR spectrometer can be utilized to establish type of bonding for to realize a new composite. The characteristic peaks in the transmittance spectrum for of PPY, NNDMA, PPY-SDS/NNDMA/OL 37 and NNDMA/PPY-SDS/ OL 37 bilayer coating are presented in figure 5. The characteristic peaks in the transmittance peaks in the transmittance spectrum for NNDMA (monomer), NNDMA/OL37 and NNDMA/PPY-SDS/OL37 coatings were presented (in figure 5b, d and f) are the following [3, 8, 20, 30-36]: in the spectrum of NNDMA, the bonds are assigned to the stretching vibration of the quinoid ring and benzenoid ring can be seen at  $1576$  and  $1483\text{ cm}^{-1}$ . The peak at about  $1228\text{ cm}^{-1}$  is assigned to C-N stretching in aromatic amines. The peak appearing near  $1342\text{ cm}^{-1}$  is attributed to the C-H stretching of  $\text{CH}_3$  group. A band at approximately  $1164$ ,  $990$  and  $746\text{ cm}^{-1}$  are attributed to the in plane and out plane C-H of the aromatic rings.



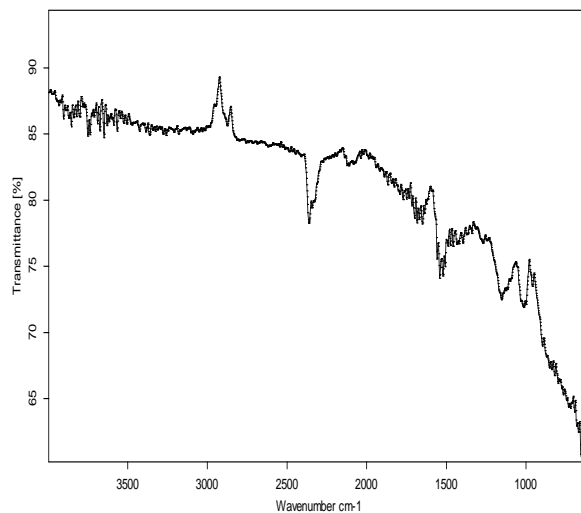
a) PPY-monomer



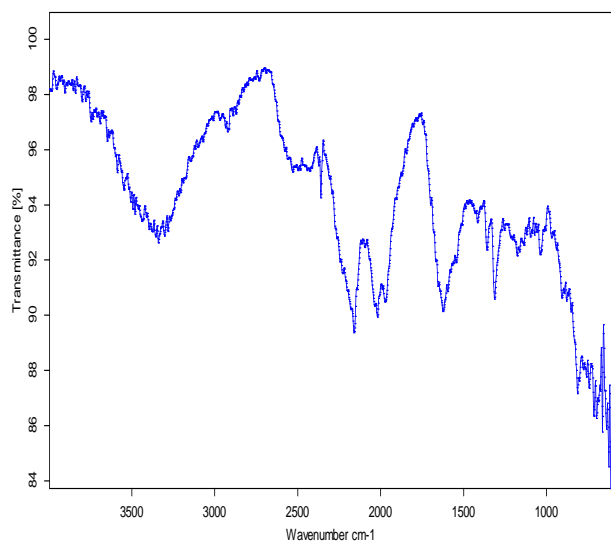
b) N,N, Dimethylaniline-monomer



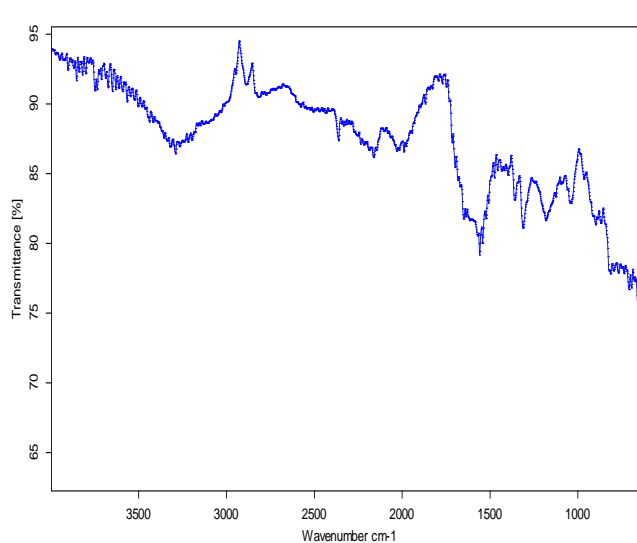
c) PPY-SDS/OL 37



d) NNDMA/OL 37



e) PPY-SDS/NNDMA/OL 37



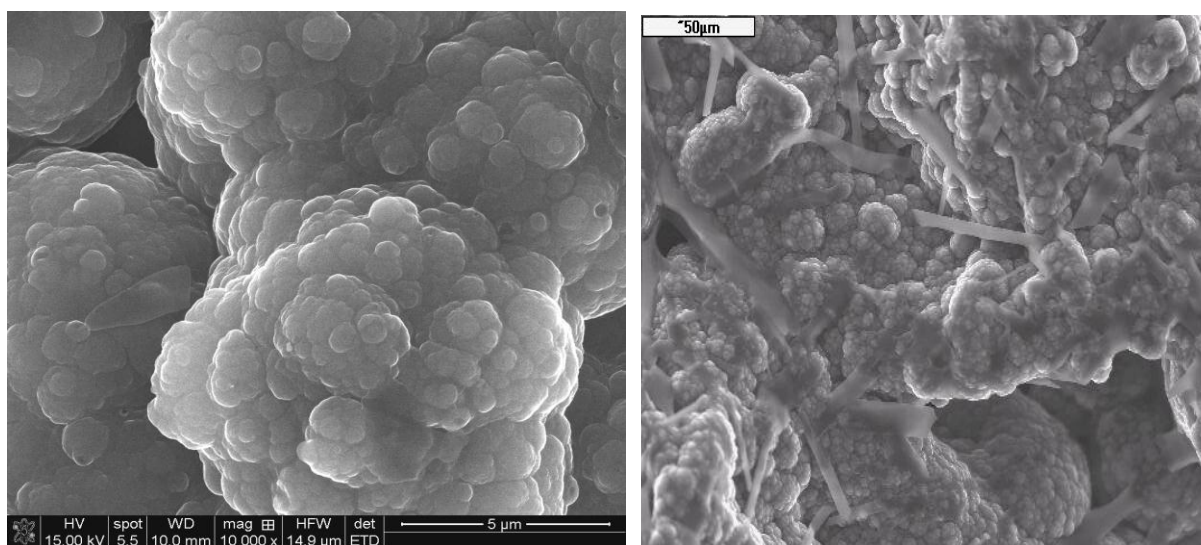
f) NNDMA/PPY-SDS/OL 37

**Figure 5.** FT-IR Spectra of PPY, NNDMA, PPY-SDS/NNDMA and NNDMA/ PPY-SDS electropolymerization on OL3 7 electrodes at galvanostatic technique.



The FT-IR spectrum of NNDMS/OL37 and NNDMA/PPY-SDS/OL37 is presented in figure 5d and 5f. The presence bands located at 1540, 1537, 1481 and 1488  $\text{cm}^{-1}$  is shown in stretching vibration of quinoid and benzoid rings. A small band at 3420  $\text{cm}^{-1}$  and 3431  $\text{cm}^{-1}$  as a result N-H stretching vibration propose the existence of N-H group in N, N dimethylaniline items, the peaks at 1310 and 1316  $\text{cm}^{-1}$  represents C-N stretching vibration in aromatic amine. A peak at about 1340 and 1348  $\text{cm}^{-1}$  is attributed at the C-H stretching of  $\text{CH}_3$  group. The existence of replaced aromatic rings showing the polymer obtained is proved by the peaks at 844 and 839  $\text{cm}^{-1}$ . A band about at 1000 and 708  $\text{cm}^{-1}$  is attributed to the in and out plane CH of the aromatic group. In the FT-IR spectrum of the NNDMA/PPY-SDS/OL37 bilayer coating the existence of the peaks at 1596, 1488 and 1316  $\text{cm}^{-1}$  is showed that NNDMA can be coated on PPY-SDS [3, 7, 30-35, 38-40].

The structure of PPY monomer, PPY-SDS and PPY-SDS/NNDMA polymers electrodeposited on carbon steel were analyzed by FT-IR. The FT-IR spectrum of PPY-SDS/OL37 and PPY-SDS/NNDMA/OL37 is shown in figure 5a, c and 5e. The main characteristic bands to the aromatic ring in PPY is visible at 1529 and 1468  $\text{cm}^{-1}$  for C=C stretching, being clearly observed. The peak at 1206  $\text{cm}^{-1}$  corresponds to the C-N stretching vibration of the pyrrole ring. The bands at 1383, 1314  $\text{cm}^{-1}$  are attributed to stretching vibration of the pyrrole ring, the sharp band located at 1676, 1624  $\text{cm}^{-1}$  is related to the C=C stretching mode. The peaks corresponding to in plane and out of plane of the N-H chains at 1074, 1141, 1177, 612 and 615  $\text{cm}^{-1}$  are observed in the composite. The peaks can be seen at 836, 881 and 972  $\text{cm}^{-1}$  is assigned to out of plane vibrations of C-H bands of doped PPY in  $\text{H}_2\text{C}_2\text{O}_4$  solution. The peak at approximately 1206, 1215  $\text{cm}^{-1}$  is due the existence of the carboxyl group of the dopant in the polymer film. The peaks at 2943, 2903  $\text{cm}^{-1}$  correspond to the aliphatic C-H stretching vibration of the  $\text{CH}_2$  and  $\text{CH}_3$  groups in the dodecylsulphate anion. In the FT-IR spectrum of the PPY-SDS/NNDMA/OL37 bilayer coating the existence of the peaks at 2943, 2855 and 1047  $\text{cm}^{-1}$  is showed that PPY can be coated on NNDMA [7, 29, 30, 36-41].



a)

b)



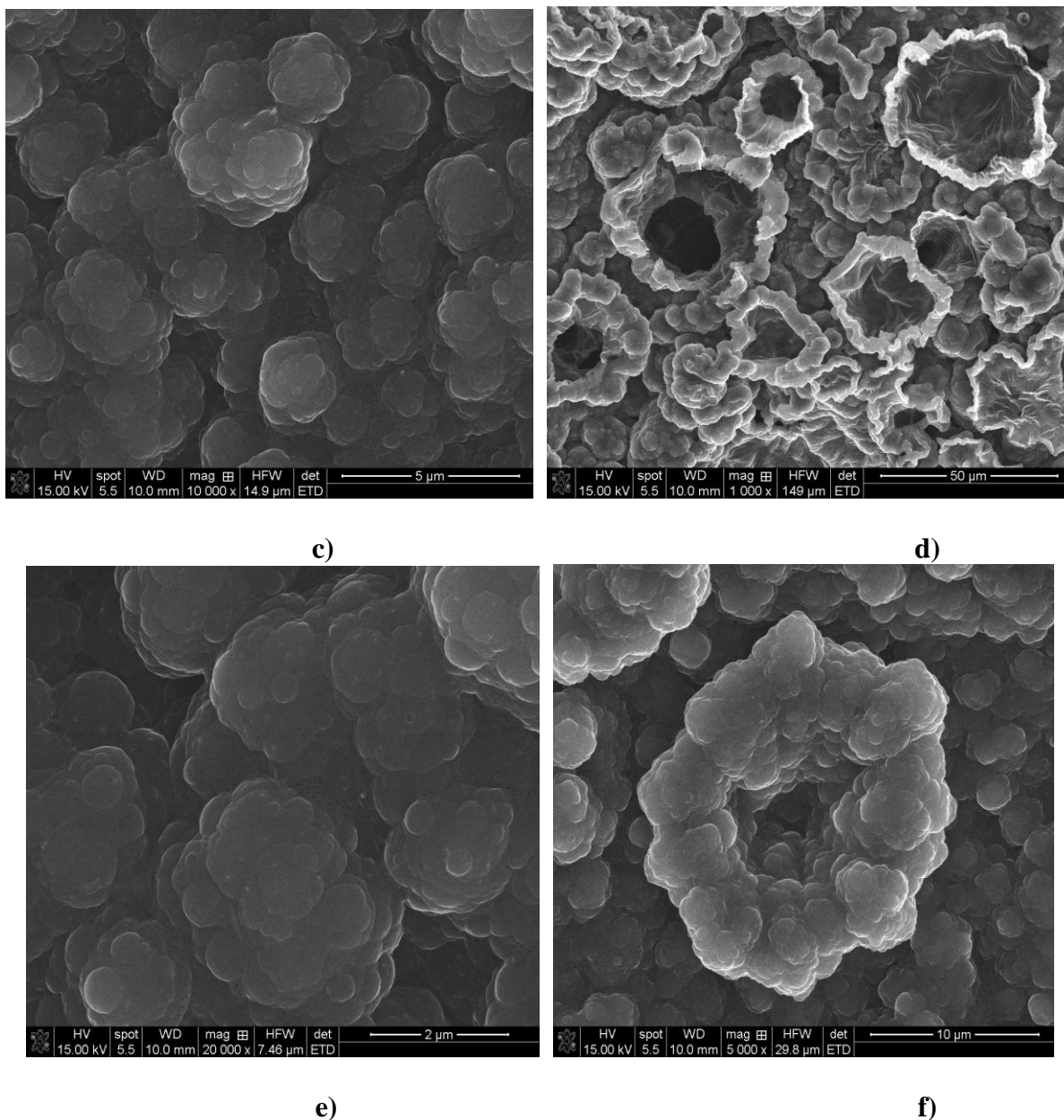


**Figure 6.** SEM images of carbon steel type OL37 electrode coated with a)PPY-SDS/OL37, b) NNDMA/OL 37, c) NNDM/PPY-SDS/ OL 37, d)PPY-SDS/NNDMA/ OL 37 before a, b, c and e and after d and f immersion in 0.5M  $\text{H}_2\text{SO}_4$

Utilizing scanning electron microscopy (SEM) measurements, the morphology structure of the polymer coatings obtained on the carbon steel OL 37 substrate was investigated. The SEM images of PPY-SDS/OL37, NNDMA/OL37, NNDM/PPY-SDS/OL37, PPY-SDS/NNDMA/OL37 coatings deposited on carbon steel are presented in figure 6.

It clearly reveals that these coatings are a homogeneous, smooth and a uniform film. The properties of the PPY-SDS coated OL 37 electrode is depicted in figure 6a and evidenced homogeneous, as cauliflower morphology specific feature to PPY formed by micro spherical grains with dimensions 5 $\mu\text{m}$  to 50  $\mu\text{m}$  in thickness. The SEM of NNDMA/OL37 film is presented in figure

6b, as shown that in this case the obtained polymeric film has a morphological structure constituted from uniform distributed polymeric chains which demonstrates the formation of NNDMA polymeric film [3, 7, 27, 28, 40-46]. It can be seen from figure 6c the film of NNDMA coated on PPY-SDS/OL 37 electrode is slightly thinner than the one in the PPY composite. In the case of PPY-SDS coated on NNDMA/OL37 bilayer polymeric film, it has as cauliflower morphology structure (from figure 6e) that is different from NNDMA morphology, which is comparable with the literature [3, 7-10, 20, 27-29, 40-46].

The coating is smooth, resistant, adherent on the OL 37 electrode. The quality of the composite is higher, having no cracks showing on the composite coating. It can be seen at figure 6 where of PPY-SDS/NNDMA and NNDMA/PPY-SDS bilayer coating is uniform, on the carbon steel type OL 37 surface and with a perfect condition of the coating. After immersion in 0.5M H<sub>2</sub>SO<sub>4</sub> solution, apparent modification in the structure morphology of the polymer coating has appeared from the electrochemical polarization techniques. As observed in the SEM pictures –6d and f, what show the diffusion of aggressive ions in the polymeric coatings [4, 7, 8, 11, 28-34, 41-42].

The corrosion performances of the obtained PPY-SDS/OL37, NNDMA/OL 37, NNDM/PPY-SDS/OL 37 and PPY-SDS/NNDMA/ OL 37 films have been analyzed in 0.5M H<sub>2</sub>SO<sub>4</sub> by potentiodynamic polarization studies and electrochemical impedance spectroscopy. Investigation of the Tafel plots at figure 7 show as the electrochemical parameters of uncoated area of OL 37 electrode and their comparison with the electrochemical parameters from coated area of carbon steel electrode in 0.5M H<sub>2</sub>SO<sub>4</sub> solutions. The coated surfaces were shown to have important decrease in corrosion current density whichever showed reduction of the cathodic and anodic reactions. It can be seen from figure 7 that the current density of cathodic Tafel branch of NNDM/PPY-SDS/OL 37 and PPY-SDS/NNDMA/ OL 37 coated carbon steel decreases considerably compared to uncoated carbon steel OL3. Anodic polarization curve from figure 7 indicate that the current density increases as a result to dissolution the electrodes at the starting of anodic polarization and afterwards, the current density decreases due to passivation of the electrode [8, 28, 41-49].

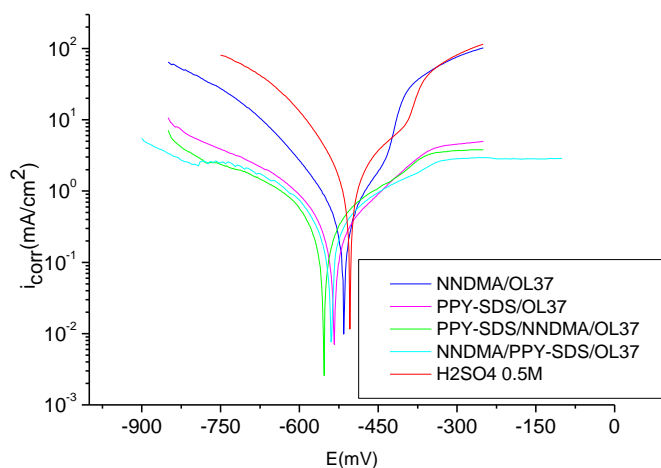


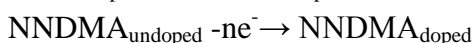
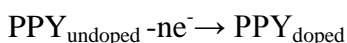
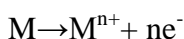
**Figure 7.** Polarization curves obtained in 0.5M H<sub>2</sub>SO<sub>4</sub> solution for uncoated and NNDMA, PPY-SDS-monolayer and PPY-SDS /NNDMA, NNDMA/PPY-SDS-bilayer coated carbon steel type of OL 37 electrodes

The electrochemical parameters as: corrosion potentials ( $E_{\text{corr}}$ ), corrosion current density ( $i_{\text{corr}}$ ), anodic and cathodic Tafel slopes obtained by the extrapolation of linear portions of the cathodic and anodic Tafel plots of carbon steel electrode coated and uncoated are presented in table 1. It can be seen from table 1, corrosion potential of coated surface of OL37 are shifted to more negative potential as compared to those of uncoated surface of OL 37 electrode. As the monolayer coatings have been compared, the PPY-SDS coating has a greater anticorrosive efficiency and the lowest corrosion current density than the NNDMA coating, because the polymer PPY film was doped with anionic surfactant of type SDS (sodium dodecyl sulfate). The use of large anions increases the anticorrosion protection of the PPY film by hindering the penetration of aggressive ions. The corrosion protection can be demonstrated by the fact that the anionic surfactant (SDS) competitively adsorbs on the OL 37 surface blocking the active sites and hence the  $\text{SO}_4^{2-}$  anion is prevented from reaching the OL37 surface and anticorrosion protection is obtained [5, 10, 11, 36, 37, 40-44]. Between the protective coatings, the NNDMA/ PPY-SDS/OL37 bilayer has the higher polarization resistance and the lowest rate corrosion and corrosion current density than PPY-SDS/ NNDMA/OL37 bilayer.

Corrosion behavior of PPY-SDS/NNDMA/OL 37 and NNDMA/PPY-SDS/OL 37 coated carbon steel electrode indicated that the polymer coated electrode had significantly greater anticorrosion performance and decreased corrosion rate compared to uncoated OL 37 electrode. These decreases in current and corrosion rate demonstrate that this monolayer and bilayer polymeric coatings prevent the cathodic and anodic process. The corrosion rate of PPY-SDS/NNDMA/OL 37 and NNDMA/PPY-SDS/OL 37 coated carbon steel has been proved to be ~10 times smaller in comparison with the uncoated carbon steel OL 37. It has been obvious that the composite coatings have prevented the action of the aggressive ions (0.5 M  $\text{H}_2\text{SO}_4$ ) on OL 37 surface. It can be observed from the polarization curves (figure 7) for PPY-SDS/NNDMA/OL 37 and NNDMA/PPY-SDS/OL 37 mono and bilayer films coated carbon steel OL 37 show that these coatings inhibit the anodic dissolution of metal (Fe) in the aggressive solution ( $\text{H}_2\text{SO}_4$ ) [7,8,10, 28, 30, 34-37]. Analyzing table 1 and figure 1 it can be seen that these coatings (NNDMA, PPY-SDS) are efficient to give protection to carbon steel electrode in 0.5M  $\text{H}_2\text{SO}_4$  medium. The corrosion mechanism of OL37 in  $\text{H}_2\text{SO}_4$  solution could occur thus [46-53]:

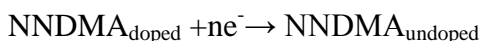
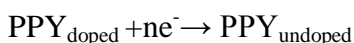
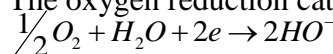
-dissolution of Me as anodic reaction

Anodic reactions:

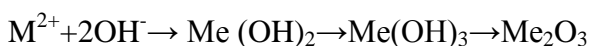


Cathodic reactions:

The oxygen reduction cathodic reaction by equation:



Chemical reactions:



The porosity of these coatings (NNDMA, PPY-SDS) is a significant characteristic for establishing when a coating is applicable or not for protection. The porosity of the coatings was calculated with the following relation [51]:

$$P = \frac{R_p(\text{uncoated})}{R_p(\text{coated})} 10^{-(|\Delta E_{\text{corr}}|/\beta_a)}$$

P is total porosity,

$R_p$ - the polarization resistance for uncoated and coated electrodes

$\Delta E_{\text{corr}}$ -the difference between corrosion potential and  $\beta_a$  is the anodic Tafel slope for uncoated OL 37 electrode.

It can be seen from table 1 that the porosities of monolayer (NNDMA, PPY-SDS) and bilayer (PPY-SDS/NNDMA and NNDMA/PPY-SDS) are 0.168, 0.083, 0.054 and 0.056.

The considerably smaller sizes of the porosity in the bilayer PPY-SDS/NNDMA and NNDMA/PPY-SDS coatings in comparison with the respective monolayer NNDMA, PPY-SDS coatings allow considerable improvement of the anticorrosive performance by preventing the access of the aggressive solution on the OL 37 surfaces [10, 35, 38].

**Table 1.** Electrochemical corrosion parameters of coated and uncoated of carbon steel OL 37 electrode in 0.5M H<sub>2</sub>SO<sub>4</sub> solutions at 25°C

	$E_{\text{corr}}$ (mV)	$i_{\text{corr}}$ (mA/cm <sup>2</sup> )	$R_p$ ( $\Omega\text{cm}$ )	$R_{\text{mpy}}$	$P_{\text{mm/ye}}$ ar	$b_a$ (mV/decade)	$b_c$ (mV/decade)	E (%)	%P
OL37 + 0.5 M H <sub>2</sub> SO <sub>4</sub>	-506	1.095	14.16	511	11.61	101	83	-	
NNDMA/OL37 monolayer	-518	0.216	64.03	104.4	2.65	83	-88	80	0.168
PPY-SDS/OL37 -monolayer	-535	0.196	87.61	94.73	2.41	111	-99	82	0.083
PPY-SDS/NNDMA/OL37- bilayer	-554	0.179	85.92	86.51	2.195	104	-94	84	0.054
NNDMA/PPY-SDS/OL37- bilayer	-553	0.153	85.01	73.95	1.877	96.5	-89	86	0.056

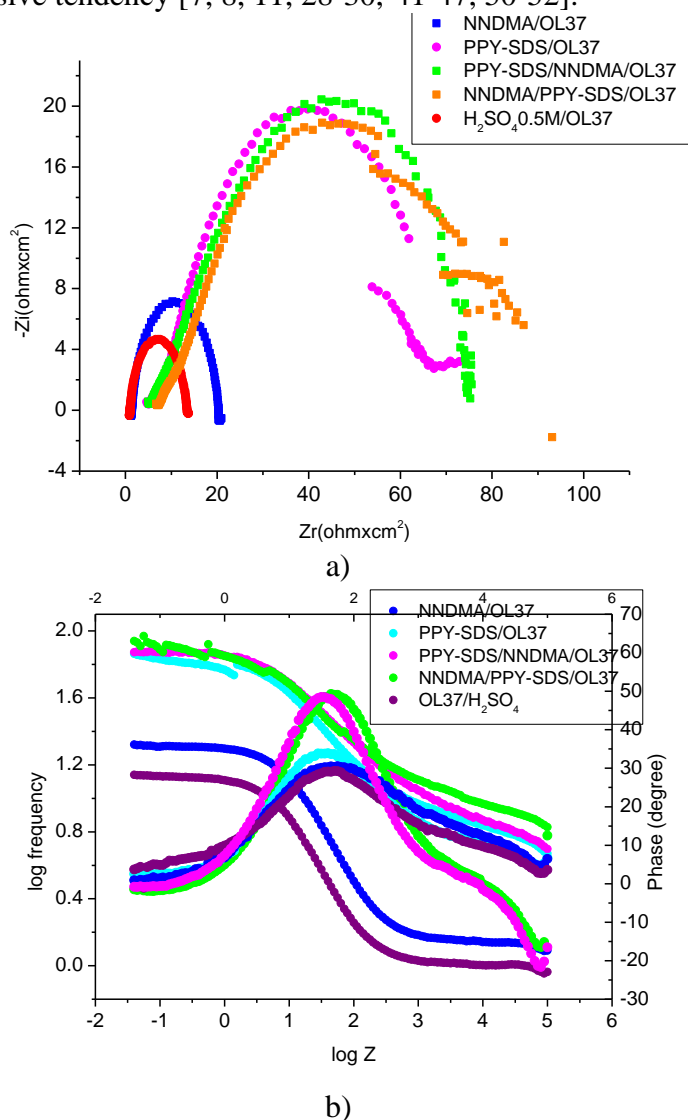
The corrosion behavior of carbon steel type OL 37 in 0.5 M H<sub>2</sub>SO<sub>4</sub> with and without of composite coatings were analyzed by electrochemical impedance spectroscopy (EIS) at the OCP condition on the frequency interval at 100 kHz and 40 mHz with an AC wave of  $\pm 10$  mV (peak-to-peak) [7, 8-11, 40-47]. EIS techniques give details about investigating the anticorrosive properties of a polymeric film as a protective film at metal corrosion. The Nyquist diagrams (figure 8) presents only one “semicircle” and the diameter of the semicircle increases while with increasing of composite coatings (bilayer coatings), assuming as the obtained protective film has been consolidated by the adding of bilayer composite coatings.

Figure 8a also show that the shape of the capacitive loops with composite polymer coatings are much higher than without coatings, assuming that these composite coatings has the best anticorrosive properties over the carbon steel type OL37 in 0.5 M H<sub>2</sub>SO<sub>4</sub>. In this paper for all the coatings studied, the electrochemical impedance spectra are analyzed by one semicircle, at a high frequency capacity loop and at low frequency inductive loop. But, these capacitive loops are not exact semicircles and this

fact is attributed to frequency dispersion, largely attributed to rugosity and inhomogeneities of the metal surface. Figure 8a likewise showed that the diameters of the capacitive loops in the presence of polymer coatings type PPY-SDS/OL37 are greater than those in the presence of coatings type NNDMA/OL37 demonstrating that these coatings have best anticorrosive effect on the OL37 in 0.5 M H<sub>2</sub>SO<sub>4</sub>, because, we used of large anion (of the anionic surfactant-SDS) which increase the anticorrosive effect of the PPY film [7, 8, 11, 22-28, 40-48].

It can be seen from figure 8a, that the diameter of capacitive loops with PPY-SDS /NNDMA and NNDMA/PPY-SDS bilayer coated carbon steel are higher than those NNDMA, PPY-SDS monolayer coated carbon steel, indicating that the bilayer coatings demonstrated better corrosion protection performances than monolayer polymer coatings.

Bode diagrams are depicted in figures 8b are in agreement with Nyquist diagrams. It can be seen that in absence of polymer coatings the electrode indicates one time constant which according to a phase angle at approximate 25° at medium and small frequencies, this case show an inductive behaviour with low diffusive tendency [7, 8, 11, 28-30,-41-47, 50-52].



**Figure 8.** EIS diagrams a) Nyquist plots and b) Bode plots for uncoated and NNDMA, PPY-SDS, PPY-SDS /NNDMA, NNDMA/PPY-SDS-bilayer coated carbon steel type of OL 37 electrodes

Contrariwise, in the presence of the polymer coatings, at the curve: phase angle depending on the frequency logarithm displays a maximum very well established assigned at a phase angle of approximate  $55^\circ$  meaning that in this situation the samples have a higher capacitive behavior, in agreement with the Nyquist diagrams. From figure 8b it can be observed that PPY-SDS /NNDMA and NNDMA/PPY-SDS-bilayer coated carbon steel OL 37 has a large frequency interval at  $55^\circ$  in comparison with the uncoated OL37 electrode at  $25^\circ$ . This is due to the strength of polymer coating counter penetration of aggressive  $H_2SO_4$  ions. Examining the Nyquist curves, it could be said that at low and medium frequencies on the plots displays a small diffusive branch with the very large capacitive loops from high frequencies interval. This case demonstrates over again that these polymer coatings ensure best anticorrosion protection [7, 8-12].

#### 4. CONCLUSIONS

In this study, we have obtained a new composite coating on OL 37 by galvanostatic deposition (layer by layer) of N, N' dimethylaniline and pyrrole- SDS in  $H_2C_2O_4$  medium.

The FT-IR technique demonstrates which the electrodeposition of NNDMA/PPY-SDS/OL37 and PPY-SDS/NNDMA was achieved and reveal to the oxidized form of N, N' dimethylaniline and pyrrole over OL37 sample.

The SEM micrographs of the PPY-SDS/NNDMA and NNDMA/PPY-SDS coatings electrodeposited on OL37 is uniform, adherent, resistant, homogeneous, smooth on the OL 37 surface and with a perfect condition of the coating.

The corrosion rate PPY-SDS/NNDMA and NNDMA/PPY-SDS coated carbon steel is proved to be ~10 times is proved than that which can be seen for uncoated carbon steel.

The electrochemical studies demonstrated that the PPY-SDS/NNDMA and NNDMA/PPY-SDS works as a corrosion protective film on OL37 in 0.5M  $H_2SO_4$  solution.

Bilayer coatings (PPY-SDS/NNDMA, NNDMA/PPY-SDS) revealed better anticorrosive efficiency than monolayer coatings (PPY-SDS, NNDMA).

The new nanocomposite realized by this method is promising and could result to industrial applications in the protection of the carbon steel substrates to corrosion.

The corrosion protection efficiency follows the order: NNDMA/PPY-SDS > PPY-SDS/NNDMA > PPY-SDS > NNDMA because the presence of these coatings causes a significant decrease in corrosion rate.

#### References

1. D. Gopi, K.M. Govindaraju, L. Kavitha, and K. Anver Basha, *Prog.Org.Coat*, 71 (2011) 11–18
2. B. A. Abd-El-Naby, O. A. Abdullatef, E. Khamis, W. A. El-Mahmody *Int. J. Electrochem. Sci.*, 11(2016)1271-1281
3. T. Ozyilmaz, N. Çolak, G. Ozyilmaz, M. K. Sangün, *Prog. Org. Coat.* 60 (2007) 24-32
4. B. Zeybek, N.O.Pekmez and E.Kilic, *Electrochim Acta*, 56 (2011) 9277-9286.
5. Nuran Özçiçek Pekmez, Kübra Cinkıllı, Bülent Zeybek, *Prog.Org.Coat*, 77 (2014) 1277-1287

6. D. Sazou, M. Kourouzidou, E. Pavlidou, *Electrochim. Acta*, 52 (2007) 4385
7. A. Yagan, N.O. Pekmez, A. Yildiz, *Electrochim. Acta*, 53 (2008) 2474
8. F. Branzoi V. Branzoi, *Rev.Roum.Chim.*, 58 (2013) 49-581
9. V. Branzoi, F. Branzoi, L. Pilan, *Mol.Cryst.Liq.Cryst.*, 446 (2006) 305-318
10. B.Duran, M.C.Turhan, G Bereket and A.S Sarac, *Electrochim Acta*, 55 (2009) 104-112
11. V.Branzoi, A. Pruna, F.Branzoi, *Mol.Cryst.Liq.Cryst*, 485 (2008) 105 -113
12. Haifeng Hu, Mengyu Gan, Jun Yan, Li Ma, Chengqiang Ge, *Prog.Org.Coat*, 81 (2015) 87-92
13. Mahmoud A. Hussein\*, Salih S. Al-Juaid, Bahaa M. Abu-Zied, Abou-Elhagag A. Hermas' *Int. J. Electrochem. Sci.*, 11 (2016) 3938-3951
14. O. Grari, A. Et Taouil, L. Dhoubi, C.C. Buron, F. Lallemand, *Prog.Org.Coat*, 88 (2015) 48-53
15. S. Jafarzadeh, P. M. Claesson, P.E. Sundell, E. Tyrode, J. Pan, *Prog.Org.Coat.*, 90 (2016) 154-162
16. Y. Dai, F. Zhu, H. Zhang, H. Ma, W. Wang, J.Lei, *Int. J. Electrochem. Sci.*, 11 (2016) 4084-4091
17. Jinqiu Xu, Yanqing Zhang, Dongqin Zhang, Yongming Tang, Hui Cang, *Prog.Org.Coat*, 88 (2015) 84-91
18. Mahmoud A. Hussein\*, Salih S. Al-Juaid, Bahaa M. Abu-Zied, Abou-Elhagag A. Hermas, *Int. J. Electrochem. Sci.*, 11(2016) 3938-3951
19. M.B. González, S.B. Saidma, *Prog.Org.Coat*, 78 (2015) 21-27
20. F. Branzoi, V. Branzoi, *Open Journal of Organic Polymer Materials*, 5 (2015) 89-102
21. B. A. Abd-El-Nabey, O. A. Abdullatef, G. A. El-Naggar, E. A. Matter and R. M. Salman, *Int. J. Electrochem. Sci.*, 11(2016) 2721-2733
22. A.Popova, M.Christov, *Corros. Sci.*, 48 (2006) 3208
23. B. Zeybek, E. Aksun, *Prog. Org. Coat*, 81 (2015)1-10
24. Abdollah Omrani, Hussein Rostami, Razieh Minaee, *Prog. Org. Coat* 90 (2016) 331–338
25. Layla A. Al Juhaiman, *Int. J. Electrochem. Sci.*, 11 (2016) 1621-1631
26. N.T.I Hien, B. Garcia, A. Pailleret, C. Deslouis, *Electrochim. Acta*, 50 (2005) 1747-1756
27. A .Kumar Singh, A Kumar Singh,E.E.Ebenso, *Int. J. Electrochem. Sci.*, 9 (2014) 352-364
28. Yağan, N. Ö. Pekmez, A. Yildiz, *Corros. Sci.*, 49 (2007) 2905-2919
29. V. Branzoi, F. Branzoi, L. Pilan, *Mat. Chem Phys.*, 118 (2009) 197-203
30. R.Hasanov, S.Bilgic, *Prog. Org. Coat*, 64 (2009) 435-445
31. Yağan, N. Ö. Pekmez, A. Yildiz, *Surf. Coat. Technol*, 201 (2007) 7339–7345
32. F. Branzoi, V. Branzoi, A. Musina, *Prog. Org. Coat* 76 (2013) 632– 638.
33. F. Branzoi, V. Branzoi, A. Musina, *Sur. Interf. Anal.*, 44 (2012) 1076-1081
34. AT Ozyilmaz, M Erbil, B Yazici, *Thin Solid Films*, 496 (2006) 431 – 437
35. A.M.Kumar, N Rajendran, *Surf. Coat. Technol*, 213 (2012), 155–166
36. V. Shinde, A.B. Gaikwad, P. Patil, *Appl. Surf. Sci.*, 253 (2006) 1037-10450
37. A Yagan, N. Pekmez, A. Yildiz, *Electrochim. Acta*, 53 (2008) 5242-5251
38. Ghadim, Morteza Farkhondekalam, A. Imani, G. Farzi, *Journal of Nanostructure in Chemistry*, 2014.
39. V. Shinde, A. B. Gaikwad, P.P. Patil *Surf. Coat. Technol*, 202 (2008) 2591-2602
40. A.K. Singh, M.A. Quraishi, *Corros. Sci.*, 52 (2010) 1373–1385
41. S Chaudhari, PP Patil, *Electrochimica Acta* 55 (2010) 6715-6723
42. D. Sazou, C. Georgolios, *Journal of Electroanalytical Chemistry*, 429 (1997) 81
43. B. Malhotra, R. Singhal, *Pramana*, 61 (2003) 331.
44. J.-C. Vidal, E. Garcia -Ruiz, J.-R. Castillo, *Microchimia Acta*, 143 (2003) 93.
45. T. Zhang, C.L. Zeng, *Electrochim. Acta*, 50 (2005) 4721.
46. D. Sazou, M. Kourouzidou, E. Pavlidou, *Electrochim. Acta*, 52 (2007) 4385.
47. V.Brusic, M. Angelopoulos, T Graham, *J.Electrochem.I Soc.*, 144 (1997) 436.
48. G.Spinks, A.Dominis, G.Wallace, D.Tallman, *J. Solid State Electrochem*, 6 (2002) 85.
49. Davoodi, S, Honarbakhsh, G. Ali Farzi, *Prog. Org. Coat*, 88 (2015) 106-115
50. P. Herrasti, P. Ocon, *Appl. Surf. Sci.*, 172 (2001) 276



51. J.Creus, H.Mazille, *Surf.CoatTechnol.*, 130 (2000) 224.

52. F. Wang, Y. Zheng, C. Mo, C. Hu, Q. Mo *Int. J. Electrochem. Sci.*, 10 (2015) 6721-6731

© 2016 The Authors. Published by ESG ([www.electrochemsci.org](http://www.electrochemsci.org)). This article is an open access article distributed under the terms and conditions of the Creative Commons Attribution license (<http://creativecommons.org/licenses/by/4.0/>).